



HAL
open science

ANALYSIS OF THE DO₃ SUPERLATTICE IN ORDERED IRON ALUMINIUM ALLOYS BY FIM AND ATOM PROBE

H.-J. Krause-Habrock, G. Frommeyer, J. Wittig, M. Kreuss

► **To cite this version:**

H.-J. Krause-Habrock, G. Frommeyer, J. Wittig, M. Kreuss. ANALYSIS OF THE DO₃ SUPERLATTICE IN ORDERED IRON ALUMINIUM ALLOYS BY FIM AND ATOM PROBE. *Journal de Physique Colloques*, 1988, 49 (C6), pp.C6-365-C6-371. 10.1051/jphyscol:1988663 . jpa-00228160

HAL Id: jpa-00228160

<https://hal.science/jpa-00228160>

Submitted on 4 Feb 2008

HAL is a multi-disciplinary open access archive for the deposit and dissemination of scientific research documents, whether they are published or not. The documents may come from teaching and research institutions in France or abroad, or from public or private research centers.

L'archive ouverte pluridisciplinaire **HAL**, est destinée au dépôt et à la diffusion de documents scientifiques de niveau recherche, publiés ou non, émanant des établissements d'enseignement et de recherche français ou étrangers, des laboratoires publics ou privés.

ANALYSIS OF THE DO₃ SUPERLATTICE IN ORDERED IRON ALUMINIUM ALLOYS BY FIM AND ATOM PROBE

H.-J. KRAUSE-HABROCK, G. FROMMEYER, J.E. WITTIG* and M. KREUSS

Max-Planck-Institut für Eisenforschung, Max-Planck-Strasse 1,
D-4000 Düsseldorf, F.R.G.

*Vanderbilt University, PO Box 6309, Station B, Nashville, TN 37235,
U.S.A.

Abstract - The perfection of the ordered DO₃ structure in Fe-(20/26/30 at%)Al alloys has been studied using field ion microscopy (FIM), atom probe (AP) measurements, and transmission electron microscopy (TEM) dark field (DF) imaging. FIM images provide a means to qualitatively characterize the degree of order in these materials. However, AP surveys of [111] poles supply additional information concerning the local perfection of the DO₃ superlattice. Although the microstructure can appear completely ordered in both FIM and TEM-DF images, the AP investigations have revealed that perfect DO₃ order occurs in only limited regions (10 to 20 unit cells) while many imperfections are always present in the atomic arrangements of the DO₃ structure.

1 - INTRODUCTION

Ordered Fe Al alloys with Al contents of 20 at% < C_{Al} < 30 at% exhibit excellent soft magnetic properties such as low coercive forces, minimum hysteresis losses and large relative permeability values especially in the high frequency range [1]. In addition, the intermetallic compound, FeAl, has been considered as potential material for high temperature application. The ordered B2 (CsCl type) lattice causes a marked increase of the flow stresses and creep strength at elevated temperature. Also, Fe-Al alloys exhibit sufficient high temperature oxidation resistance from the preferential formation of stable protective alumina layers [2].

The main disadvantage of these ordered alloys is the lack of room temperature ductility. A basic understanding of the relationship between the microstructure and the inherent brittleness requires a detailed knowledge of the atomic distribution of the alloying elements within the ordered superlattices. Important factors include the domain sizes and the structure of the domain boundaries since these are considered to strongly influence the movement of dislocations.

Prior field ion microscopy (FIM) investigations of disorder - order phase transformations have predominantly studied reactions of disordered fcc lattice into the ordered L1₀ [3,4], L1₂ [5,6] and other superlattices [7,8,9]. Contrast interpretations of FIM images of binary alloys is often not straight forward because of invisibility of one of the atomic species. This can result from preferential ionization, e.g. in Pt-Co alloys where the smaller Co atoms will not be imaged [4,5], or preferential field evaporation of one substitutional atom type at a minimum evaporation field strength [10,11,12].

For the case of Fe-Al alloys, a study by Paris et al. [13] has concluded that Fe is the imaging species while the Al atoms are invisible. Previous work by the current authors [9], which combined FIM imaging with atom probe (AP) analysis of DO₃ ordered Fe₃Al type alloys, has unambiguously shown that this effect is caused by preferential field evaporation of the Al atoms. For a perfect DO₃ structure, there exists a periodic arrangement in the [111] direction, AAABAAAB..., consisting of three alternating 100% Fe (111) planes followed by a pure Al (111) plane. In the [001] direction, the DO₃ ordered structure has a ABAB type stacking of 100% Fe planes and a mixed layer of 50% Fe and 50% Al atoms. Atom probe surveys of the [111] pole in Fe₃Al have shown that when the last (111) Fe plane lying above the (111) Al plane begins to evaporate, the Al atoms below evaporate together with the Fe atoms as a double layer. This is consistent with the data from the [001] poles where pure Fe and mixed Fe-Al (001) planes are observed to field evaporate together.

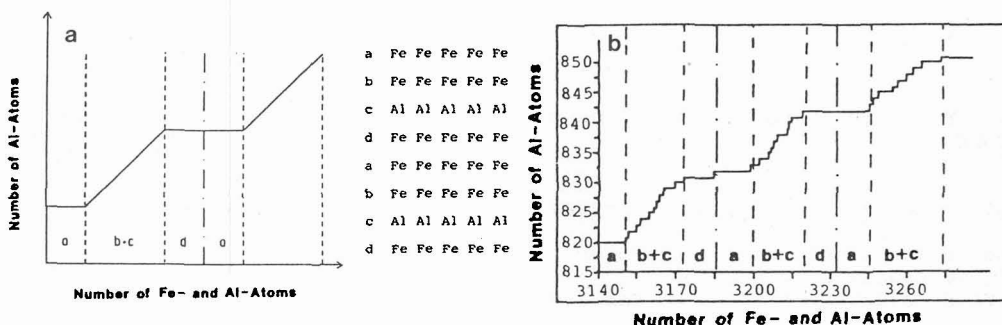


Fig. 1a - Model ladder diagram from a [111] atom probe survey of a perfectly ordered DO_3 structure assuming double evaporation of Fe and Al layers.
b - Experimental ladder diagram from an ordered DO_3 superlattice.

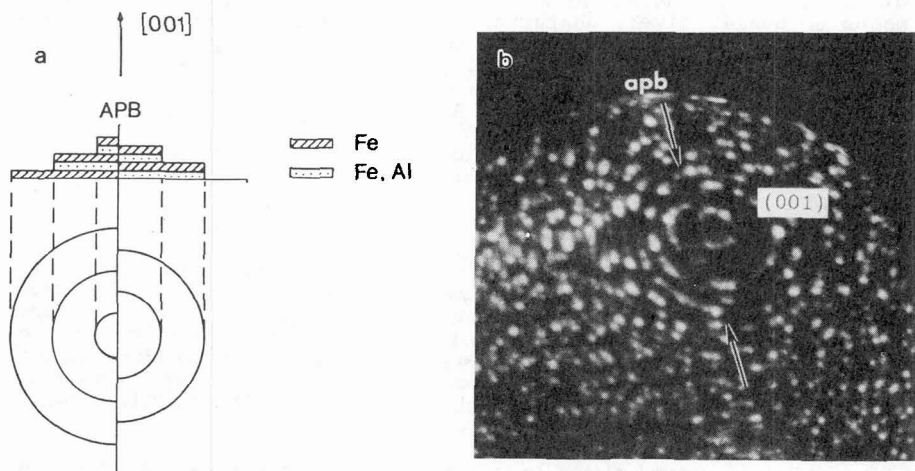


Fig. 2a - Schematic diagram of the FIM image of an anti-phase boundary (APB) on a [001] pole. Only the pure Fe planes are imaged since the mixed Fe and Al layers have preferentially evaporated.
b - FIM image of an APB on a [001] pole from a DO_3 superlattice.

The evaporation sequence of the periodicity of (111) planes allows the perfection of the DO_3 superlattice to be observed in a ladder diagram as schematically depicted in [figure 1a](#) and experimentally in [figure 1b](#). First a pure Fe plane is detected, then comes a mixed Fe and Al double layer, and finally two pure Fe planes are observed as a horizontal step in the diagram. Preferential evaporation of the Al atoms has also explained the contrast produced by anti-phase boundaries (APB) in the DO_3 superlattice. [Figure 2a](#) is a schematic representation of an APB on a [001] pole. Only the Fe layers are imaged as semi-circular rings since the mixed Fe-Al layers will have preferentially evaporated. These have been experimentally observed only on the [001] pole as shown in [figure 2b](#).

In the current paper, the atom probe technique is used to study the perfection of DO_3 ordering in Fe-Al alloys with Al concentration of 20, 26, and 30 at%. The results cannot yet express a quantitative determination of an ordering parameter. However, the extraordinary spatial resolution of the FIM-AP provides information unavailable from any other method about the local perfection of atomic ordering.

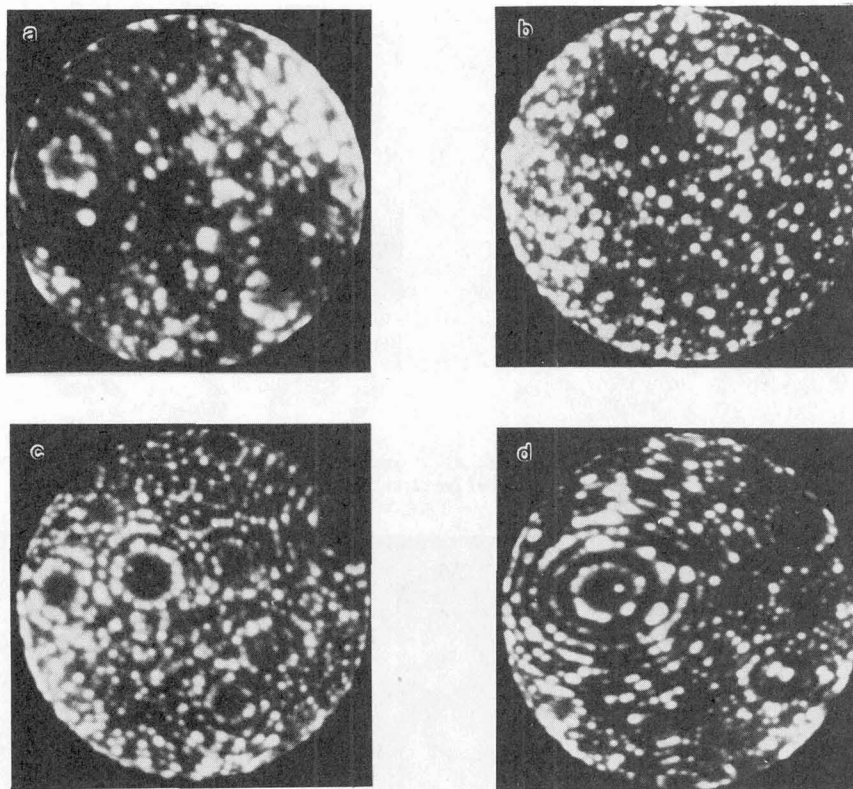


Fig. 3 - Representative FIM images of the four alloys;
 a) $\text{Fe}_{90}\text{Al}_{10}$, b) $\text{Fe}_{80}\text{Al}_{20}$, c) $\text{Fe}_{74}\text{Al}_{26}$, d) $\text{Fe}_{70}\text{Al}_{30}$.

2 - EXPERIMENTAL PROCEDURE

Four Fe-Al alloys containing 10, 20, 26, and 30 at% aluminium have been prepared by induction melting under vacuum. Samples from the ingot material were encapsulated in evacuated quartz tubes, homogenized by heat treatment at 1150 °C for 24 h and furnace cooled (4 K/min) down to room temperature. After homogenization sample blanks of the dimensions: 0.5 x 0.5 x 20 mm were cut for FIM investigations, and 2.3 mm discs, 0.4 mm thick, were taken for comparative TEM studies. These blanks were encapsulated in evacuated quartz tubes, heat treated at 1150 °C for 2 until 48 h and quenched by crushing the tubes under water. The formation of the DO_3 and B2 superlattices by the $\text{A2} \rightarrow \text{DO}_3$ and $\text{B2} \rightarrow \text{DO}_3$ transformation was promoted by annealing the samples in vacuum at 450 °C/100 h for the $\text{Fe}_{80}\text{Al}_{20}$ and $\text{Fe}_{70}\text{Al}_{30}$ material and at 400 °C for up to 250 h for the $\text{Fe}_{74}\text{Al}_{26}$ alloy. The three different compositions were chosen in order to cover the whole DO_3 phase field.

The FIM specimens were electropolished at 20 °C initially in 18 vol% perchloric acid, 18 vol% 2-butoxyethanol, and 64 vol% acetic acid at 30 V. Final polishing was performed in a 1 vol% perchloric acid and 99 vol% 2-butoxy ethanol at 20 V. FIM and atom probe analysis were carried out in an ultra high vacuum chamber, basic pressure $< 10^{-9}$ mbar, using neon imaging gas of $5 \cdot 10^{-5}$ mbar. The samples were helium cooled and the tip surfaces of the specimens were cleaned and smoothed down to the final shape by field evaporation of about 100 atom layers.

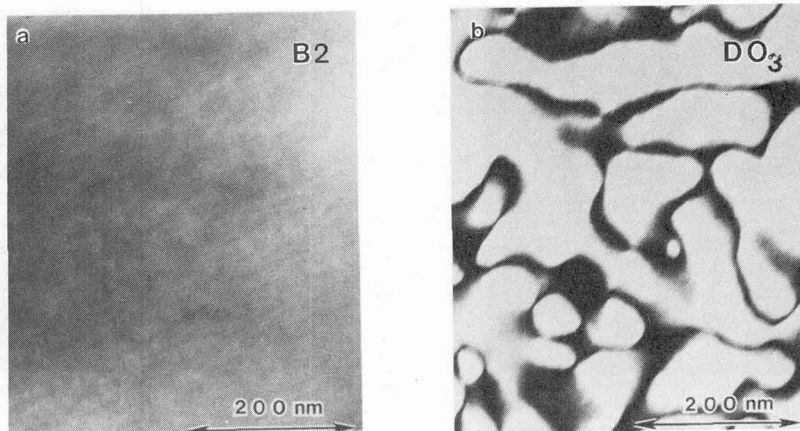


Fig. 4 - TEM dark field images of the $\text{Fe}_{70}\text{Al}_{30}$ ordered alloy using the B2 superlattice reflection in (a) and the DO_3 reflection in (b).

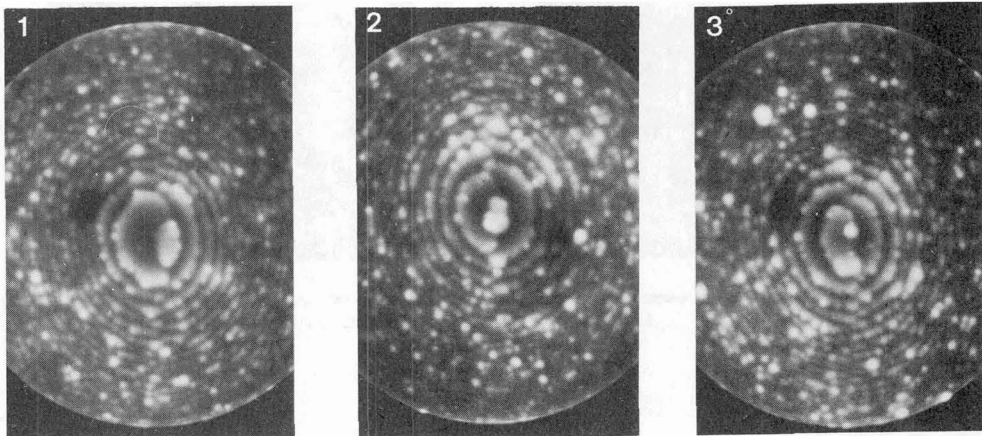


Fig. 5 - Field evaporation sequence of an APB on a [001] pole in the $\text{Fe}_{70}\text{Al}_{30}$ alloy.

3 - RESULTS AND DISCUSSION

Figures 3a-d depict representative FIM images of the four alloys with Al contents ranging from 10 to 30 at%. The images from these alloys reveal that the [001] pole is always the prominent feature. This is in contrast to higher melting point bcc metals where the [011] pole often dominates the image. As is normally the case for a substitutional solid solution, introducing 10 at% Al atoms causes a distortion of the Fe lattice and the corresponding FIM image loses its regularity in figure 1a. This effect increases at 20 at% Al where the Fe atoms which are the imaging species appear as random spots with only the [001] pole distinctly apparent. In other samples, the $\text{Fe}_{80}\text{Al}_{20}$ alloy, which lies on the edge of the DO_3 phase field, revealed a clearer image with other low index poles more evident than in this particular example.

Increasing the Al content close to the stoichiometric composition of the DO_3 superlattice in the $\text{Fe}_{74}\text{Al}_{26}$ alloy provided FIM images with crystallographic regularity and other low index poles of the Fe sublattice are now depicted in the images. This regularity is also apparent in the $\text{Fe}_{70}\text{Al}_{30}$ alloy which indicates that it as well exhibits an ordered arrangement of the Al atoms in the Fe lattice. Nevertheless, the hyperstoichiometric composition does not reveal the clarity in the FIM image that is observed in images of the stoichiometric Fe_3Al material.

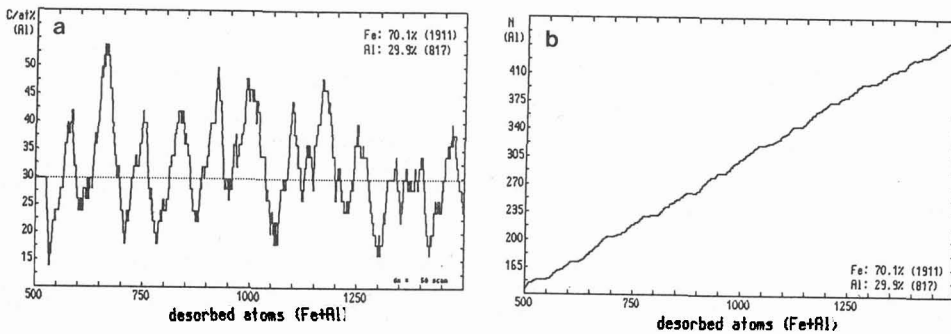


Fig. 6 - Representative section of a concentration profile in (a) and the corresponding ladder diagram in (b) from the Fe₇₀Al₃₀ alloy.

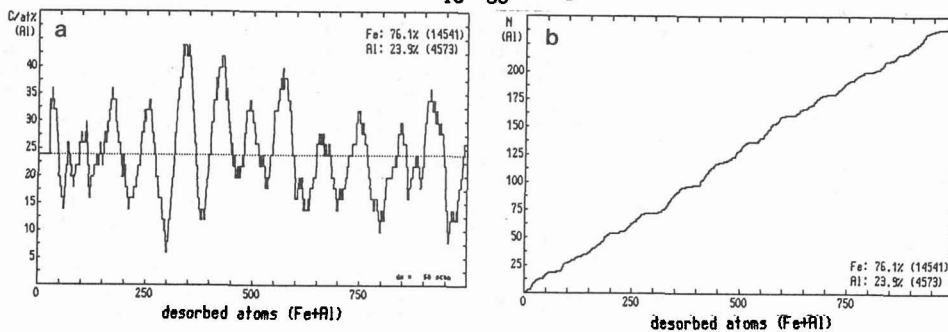


Fig. 7 - Representative section of a concentration profile in (a) and the corresponding ladder diagram in (b) from the Fe₇₄Al₂₆ alloy.

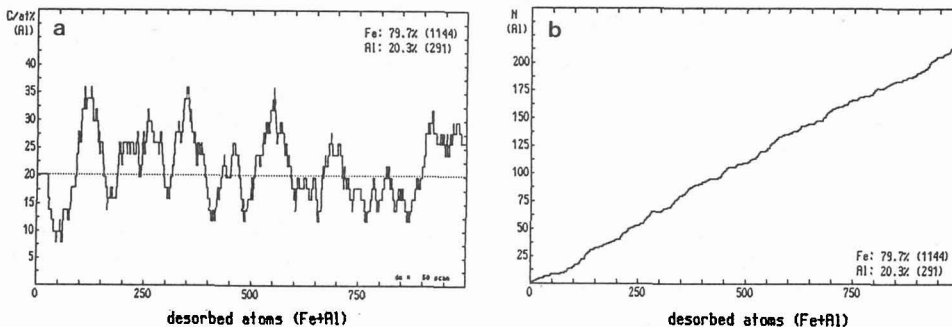


Fig. 8 - Representation section of a concentration profile in (a) and the corresponding ladder diagram in (b) from the Fe₈₀Al₂₀ alloy.

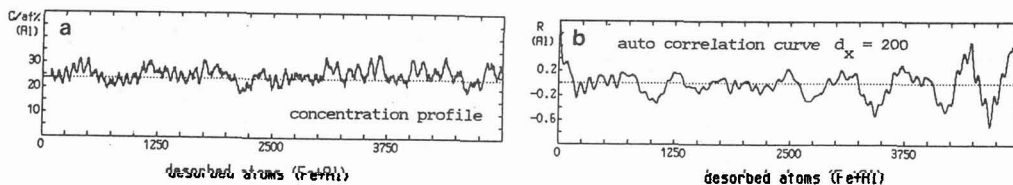


Fig. 9a - Concentration profile Fe₇₄Al₂₆ b) corresponding auto correlation curve.

Figures 4a-b are dark field (DF) transmission electron microscopy (TEM) images of the $\text{Fe}_{70}\text{Al}_{30}$ ordered alloy using B2 and DO_3 superlattice reflections respectively. In the annealed condition, the structure is completely DO_3 ordered with no evidence of APB's in the B2 DF image of figure 4a. The APB's which appear in the DO_3 DF image in figure 4b as thick blurred lines have also been detected in the FIM. Figures 5a-c are an evaporation sequence of a [001] pole in the $\text{Fe}_{70}\text{Al}_{30}$ alloy which reveals an APB. Because of the large size of the domains in this alloy, these features were rarely observed. However, in this particular case the overlapping rings of the Fe atoms (i.e. the imaging species) suggests a possible segregation of Fe atoms on this APB.

The [111] AP surveys in figures 6 - 8 are representative sections of the concentration profiles and ladder diagrams of the 30, 26, and 20 at% Al alloys which can be interpreted as a measurement of the perfection of DO_3 ordering. For the $\text{Fe}_{74}\text{Al}_{26}$ material, the fluctuations in the concentration profiles and the corresponding steps in the ladder diagrams exhibit perfect DO_3 ordering over small distances, two to three unit cells. But this perfect ordering was never detected for over more than a few unit cells before the size of the steps in the ladder diagram indicated Al atoms were occupying sites on the Fe planes, see figure 7. This result was reproducibly observed with over 9362 atoms (i.e. 312 atomic layers) measured for the $\text{Fe}_{74}\text{Al}_{26}$ alloy. Possible explanations for the lack of perfection in the ordering include non-equilibrium conditions owing to insufficient annealing times (250 h at 400 °C) or perhaps at this temperature an entropy effect promotes imperfection in the DO_3 ordered structure. Other possible causes which must be considered are the slightly non-stoichiometric composition of 26 at% Al and the chance that preferential evaporation of Al atoms from neighbouring underlying planes could be influencing the ladder diagrams.

For the $\text{Fe}_{70}\text{Al}_{30}$ alloy, the hyperstoichiometric composition produced a decrease in the size of the pure Fe steps in the [111] ladder diagrams, see figure 6. As in the 26% Al material, small regions of perfect DO_3 ordering were detected but they were fewer in number and the regions were smaller in size than for the stoichiometric Fe_3Al composition. Figure 8 depicts a representative concentration profile and ladder diagram for the $\text{Fe}_{80}\text{Al}_{20}$ material. These surveys were difficult to acquire owing to the poor imaging characteristics of the [111] poles. However, the limited data that were obtained revealed only slight indications of the ordered structure corresponding to the distorted lattice which produced the inferior imaging contrast.

Figure 9a is a complete composition profile for a $\text{Fe}_{74}\text{Al}_{26}$ sample. The total number of about 5000 atoms corresponds to 250 atomic planes or 42 nm. An interesting observation is the rather large fluctuations in the composition over long distances (8 to 10 nm). Applying an auto correlation method which removes statistical noise [14], figure 9b exhibits a long wavelength periodicity in the composition. A larger data base is required in order to get more statistical information for a significant proof of these detected long range concentration fluctuations.

4 - CONCLUSIONS

From the investigated Fe Al alloys the nearly stoichiometric $\text{Fe}_{74}\text{Al}_{26}$ alloy reveals the most perfectly ordered atomic arrangement in the FIM images. The corresponding atom probe surveys of the [111] poles show that this composition is characterized by the regular ordered structure in the ladder diagrams.

However, although the ordering appears complete in the FIM and TEM images, atom probe analysis reveals that the ordering is only locally perfect with many imperfections present in the structure.

APB's have only been observed on the [001] poles. FIM evaporation sequences suggest that segregation of Fe atoms may be present. Segregation of Fe in the APB's could correspond to the thick blurred APB's detected in the TEM.

FIM-AP technique provides a sensitive method to study the DO_3 -ordering phase in Fe-Al alloys.

Acknowledgement

The authors gratefully acknowledge the financial support from the Bundesministerium für Forschung und Technologie.

REFERENCES

- [1] C. Heck, "Magnetic Materials and their Applications", Butterworths, London 1967
- [2] G. Sauthoff, Z. Metallkde. 77 (1986) 654-666
- [3] H.N. Southworth, and B. Ralph, Phil. Mag. 14 (1966) 383
- [4] T.T. Tsong, and E.W. Müller, J. Appl. Phys. 38 (1967) 545
- [5] T.T. Tsong, and E.W. Müller, J. Appl. Phys. 38 (1967) 3531
- [6] R. Sinclair, J.A. Leake, and B. Ralph, Phys. stat. sol. (A) 26 (1974) 285
- [7] R.J. Taunt, and B. Ralph, Phys. stat. sol. (a) 29 (1975) 431
- [8] R. Grüne, A. Hütten, and L.V. Alvensleben, J. de Physique 47 (1986) 295
- [9] H.J. Krause, J.E. Wittig, and G. Frommeyer, Z. Metallkde. 78 (1987) 576
- [10] R. Wagner, "Field Ion Microscopy", Springer-Verlag, Berlin, Heidelberg, New York 1982, p. 22
- [11] R.J. Taunt, R. Sinclair, and B. Ralph, Phys. stat. sol. (A) 16 (1973) 469
- [12] R. Sinclair, B. Ralph, and J.A. Leake, Phil. Mag. 28 (1973) 111
- [13] D. Paris, P. Lesbats, and J. Levy, Scripta Met. 9 (1975) 1373
- [14] J. Piller, and H. Wendt, 29th Intern. Field Emission Symposium, Göteborg, Schweden 1982, p. 265